processes

MDPI

Article

High-Flexibility MPPT Techniques with Communication Scan Network for PV Micro-Grid System

Yu-Kai Chen [1,*], Hong-Wen Hsu [1], Chau-Chung Song [1] and Yu-Syun Chen [2]

[1] Department of Aeronautical Engineering, National Formosa University, Yunlin 600, Taiwan; hsu.kevinhw@inventec.com (H.-W.H.); ccsong@nfu.edu.tw (C.-C.S.)
[2] Fego Precision Industrial Co., Ltd., Taichung City 413, Taiwan; chen_gmezx@fego.com.tw
* Correspondence: ykchen@nfu.edu.tw

Abstract: This paper proposes the design and implementation of inductor-inductor-capacitor (LLC) converters with modules connected in series with the power scan method and communication scan network (CSN) to achieve MPPT and regulate the output voltage for the PV micro-grid system. The Dc/Dc converters includes six isolated LLC modules in series to supply ±380 V output voltage and track the maximum power point of the PV system. The series LLC converters are adopted to achieve high efficiency and high flexibility for the PV micro-grid system. The proposed global maximum power scan technique is implemented to achieve global maximum power tracking by adjusting the switching frequency of the LLC converter. To improve the system flexibility and achieve system redundancy, module failure can be detected in real time with a communication scan network, and then the output voltage of other modules will be changed by adjusting the switching frequency to maintain the same voltage as before the failure. Additionally, the proposed communication scan network includes the RS-485 interface of the MPPT series module and the CAN BUS communication interface with other subsystems' communication for the PV micro-grid application system. Finally, a 6 kW MPPT prototype with a communication scan network is implemented and the proposed control method is verified for the PV system.

Keywords: LLC; MPPT; micro-grid

Citation: Chen, Y.-K.; Hsu, H.-W.; Song, C.-C.; Chen, Y.-S. High-Flexibility MPPT Techniques with Communication Scan Network for PV Micro-Grid System. *Processes* **2022**, *10*, 117. https://doi.org/10.3390/pr10010117

Academic Editor: Luigi Piga

Received: 6 December 2021
Accepted: 3 January 2022
Published: 7 January 2022

1. Introduction

Applications with photovoltaic (PV) energy have significantly increased in the last decade, since fossil energy resources have been rapidly depleting, and PV energy is pollution-free, abundant, and broadly available [1]. As the characteristic curve of solar panels is a non-linear curve, it is necessary to carry out the maximum power tracking method, such as the disturbance observation method, increased conductivity method, constant voltage method, current sweep method, straight line approximation method, etc. [2–6]. Much of the literature has analyzed various maximum power tracking laws, and discussed the advantages and disadvantages of each law, and aspects that could be improved or refined.

In addition to the common disturbance observation method or incremental conductance method in foreign research, many types of neural network or fuzzy control have also been proposed [7], in order to increase the accuracy and stability of the solar panel when it is working at the maximum power point, for the maximum power tracking of solar panel characteristic curve deformation during solar panel shading. Many kinds of solar maximum power tracking for shading have been proposed at home and abroad. If there is particle swarm optimization [8], or it can be improved by the perturbation observation method, it can be used in shading situations. There are also studies on the maximum power-tracking method of shading [9,10]. In [11], the center point iteration MPPT algorithm is proposed for an LLC micro-converter system. Global maximum power point

tracking (GMPPT) is the process of extracting maximum power from the PV system under partially shaded conditions [12–15]. A new GMPPT method uses the maximum power point voltage, which is about 0.8 times that of the solar cell, open-circuit voltage model, which is achieved by effective partial scanning of the P-V curve [12] to improve the MPP's convergence performance. The paper presented a hybrid GMPPT algorithm for constant voltage load applications using a single current sensor [13]. The nonlinear robust controller is implemented [14,15] to achieve the GMPPT for a partially shaded PV system. This paper proposes a cost effective and fast convergence speed using the global maximum power scan (GMPS) technique based on the variable switching frequency and constant output voltage and implemented with a micro-controller.

For large-scale solar systems, there are two main configurations for grid connection: one is a centralized topology and the other is a multi-string topology [16,17]. The centralized topology is to connect diodes in series on the output side of the solar panel, and then connect multiple sets of solar panels in parallel to use a centralized converter for maximum power tracking. The other multi-series topology uses the output of each set of solar panels for conversion. Then, they are connected to the bus bar, and the maximum voltage power on each set of converters is tracked, so that each set of solar panels can output at the maximum power. The multi-string topology method is suitable for high-power and high-quality applications. In high-power applications, it reduces the load of each group of circuits and improves the overall rated power [17,18]. A high-voltage gain isolated micro-converter is proposed and implemented with a single-voltage MPPT control [19]. The proposed isolated architecture has low power and cannot be applied to large-scale solar systems. The isolated port differential power-processing architecture is presented for solar PV applications [20]. However, the system architecture is more complicated.

In this paper, we propose multiple modules in a series connection to achieve the MPPT. Each module has the maximum power-tracking method with the power scan method, six modules were connected in series to achieve 6 kW output power and the output voltage was $\pm$380 V. The number of modules and operated switching frequencies can be adjusted with the communication scan network of the designed system to achieve system flexibility and redundancy. The proposed communication scan network includes the half-duplex RS-485 interface of the MPPT series modules, and the CAN BUS communication interface with other subsystems' communication. Therefore, the global MPPT feature, high flexibility, redundancy and regulation of the output voltage of the Dc/Dc converters can be achieved with the communication scan network. In short, this paper proposes a novel method that makes full use of the advantages of the DSP chip's computing speed, and makes full use of the software to achieve a global MPPT, high flexibility and high reliability.

2. The Series-Connected Module LLC Converter

This approach can readily adapt to existing electrical facilities and expedite the use of renewable energy. However, the existing high efficiency and compact appliances and equipment are powered by dc, which is converted by rectifying an ac source with power actor correction. To use renewable energy more efficiently, dc electricity should be directly supplied to these loads. This supply scheme is very different from that of the conventional ac distribution and supply system. The configuration of the dc-distributed system with a grid connection is shown in Figure 1, in which a bi-directional inverter is introduced to regulate the dc-grid voltage within a certain range. An electronic breaker (EB) is an automatically operated electrical switch, designed to protect the devices from the damage caused by an excess current from an overload or short circuit. RS-485 communication is used to complete the communication of six solar panel modules to obtain the health information and voltage and current values of each group, as shown by the green dotted line. Additionally, CAN BUS communication can be used to complete the communication of the PV micro-grid system and obtain health information for each sub-system, as shown by the red dotted line.

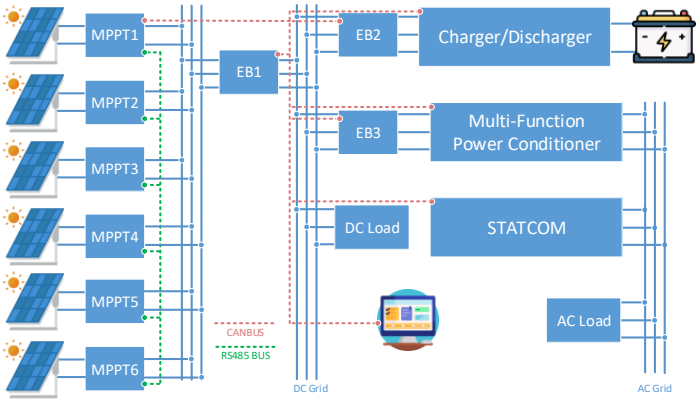

Figure 1. The proposed communication scan network for PV micro-grid system.

The positive and negative voltage three-wire output is provided to the multi-level bi-directional inverter (multi-function power conditioner) of the subsequent stage, and the first stage is LLC series-connected modules, as shown in Figure 2. Additionally, the number of modules can be adjusted with the output voltage of the system to achieve system flexibility. For example, to increase the power level, the output voltage of the large-scale grid-tied system is adopted at ±1000 V; thus, the number of modules will be increased. If the boost converter is used as the MPPT when applied to the utility power grid-tied system, it is often necessary to add a transformer to solve the leakage current problem. Therefore, the isolated soft-switching LLC converter is adopted to achieve high efficiency and eliminate the leakage current for a PV grid-tied system.

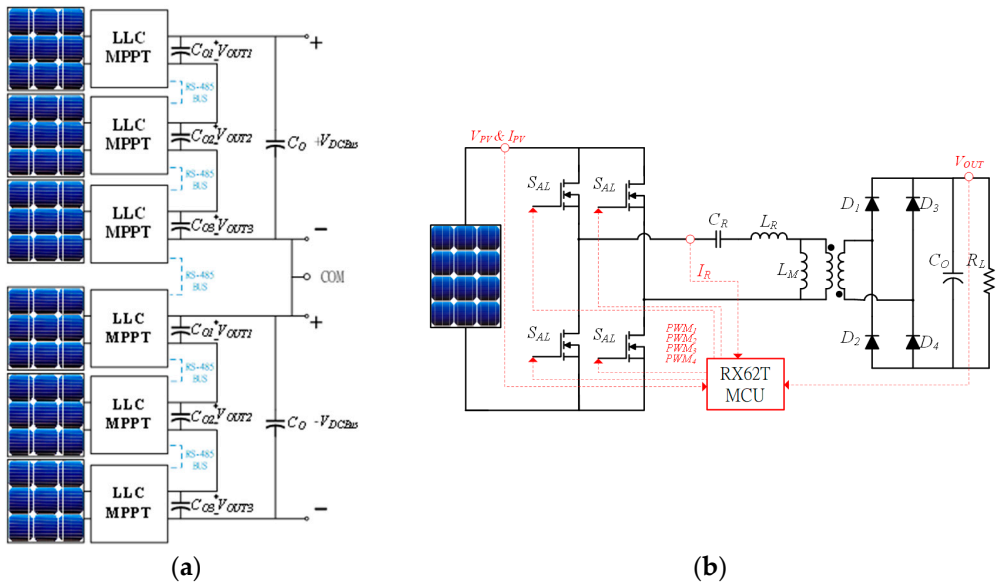

(**a**) (**b**)

Figure 2. (**a**) A module of the LLC DC/DC converter, (**b**) the system block diagram of multi-level LLC DC/DC PV system.

The output voltage of the proposed MPPT converter is controlled by the amount of current injected into an electrical power grid. The LLC resonant converter is a Dc/Dc converter with frequency control. The output voltage of its LLC resonant converter is controlled by the bi-directional multilevel inverter. When the solar power needs to be increased, the switching frequency of the LLC converter is reduced (the voltage gain is increased), and the DC bus output voltage is increased to regulate the DC bus voltage, that is, to increase the amount of current sent to the electrical power grid. However, the design of and discussions on the grid-tied inverter are not the focus of this paper.

The design and implementation of a multi-module LLC Dc/Dc PV system includes the development and implementation of multi-string interleaved converters for a maximum-power point tracker to supply three-wire DC output voltages to a grid-connected system. The system block diagram of the proposed PV system is shown in Figure 2a. The LLC converter consists of three series modules. Figure 2b shows the circuit schematic of the LLC resonant converter with a micro-controller RX-62T, which represents one module. A 6 kW multi-level LLC system with two groups of three connected modules is implemented and the the operating principle and MPPT tracking accuracy of the PV system are verified.

The design procedure of the LLC converter is listed as follows:

Step 1: Selecting the Qmax value, Q is quality factor;

Step 2: Selecting the m value, where m is the ratio of total primary inductance to resonant inductance;

Step 3: Finding the minimum normalized switching frequency;

Step 4: Voltage gain verification;

Step 5: Calculating resonant component values

where $Q = \frac{\sqrt{L_{R/C_R}}}{R_{ac}}$ is quality factor, $R_{ac} = \frac{8}{\pi^2} \times \frac{N_p{}^2}{N_s{}^2} \times R_o$, reflecting $m = \frac{L_R + L_M}{L_R}$.

From the above discussion, we can see that the LLC resonant voltage gain is required in the range from 0.875 to 1.319. The lower Q value curve can achieve a higher gain when the PV system is operated under a light load, but is less sensitive to frequency modulation and increases the switching loss. The higher Q value can reduce the switching loss but the voltage gain in the LLC resonant tank is smaller than the low Q value. Therefore, the m and Q parameters are determined to be 5.4 and 0.4 to meet the system specification, respectively. The designed proposed parameters are the resonant inductor L_R = 7.8 μH, resonant capacitor C_R = 320 nF, and magnetizing inductor L_M = 38.5 μH.

3. Global Maximum Power Scan (GMPS) Technique with Communication Scan Network

Under different irradiations, teh solar panel has different short currents. When there are lots of solar panels in series, the partial shading of one short current is lower than that of a non-shading one, causing the non-shading one to fail. To resolve this problem, we will parallel one bypass diode: when the shading panel used in short current, the other's overcurrent will flow past the bypass diode to maintain a normal solar panel output. Figure 3 shows the current flows when shading. Figure 4 shows the V-I curve and P-I curve, because the shading panel's short current will become lower, making V-I curve into two blocks. The P-I curve will have lots of Local Maximum Power Points (LGPP), but only one Global Maximum Power Point (GMPP). If there are many different irradiations in the series solar panels, the highest crest is GMPP, and the others are LMPP. Multiple crests will cause the Maximum Power Point Tracking (MPPT) to become harder and perhaps only track LGPP, not GMPP.

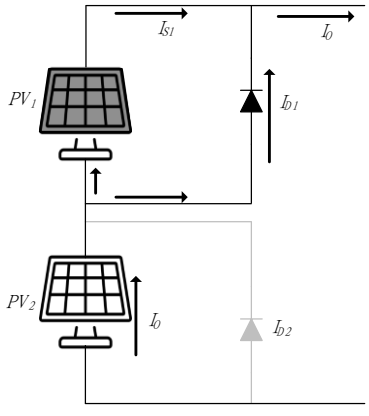

Figure 3. The current flow under shading conditions.

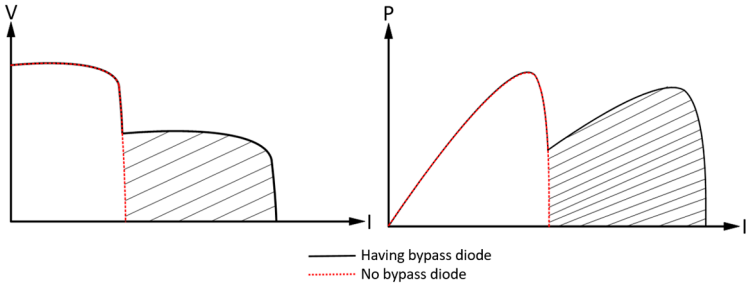

Figure 4. V-I curve and P-I curve under shading conditions.

3.1. Global Maximum Power Scan (GMPS)

P&O is a highly simple technique to vary a desired step in the duty cycle, so the solar panel's voltage and current will change. Then, the previous data and data after perturbation are compared. The P&O parameter is the switching frequency of the LLC converter to vary the converter gain and achieve MPPT. The P-V curve caused by the changing frequency method is shown in Figure 5. Firstly, we measured and compared the previous voltage and current values and the ones after perturbation. Secondly, we determined the next switching frequency of the LLC converter to increase the output power of the PV system.

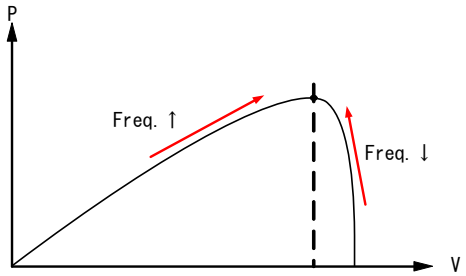

Figure 5. The P-V curve caused by changing switching frequency.

We used the global maximum power scan method to reach the global maximum power point (GMPP) for the proposed PV system. By changing the switch frequency of the LLC Dc/Dc converter, we measured the power values of the solar panel when the LLC converter was operated from a low frequency to a high frequency. Therefore, the P-V curve of the solar panel is measured and we can extract the GMPP of the solar array. Figure 6 shows the proposed scanning method, that is, the LLC converter changes the switching frequency to change its operating voltage from the voltage P_1 to P_6. After that, we can obtain a P-V curve and find the GMPP's location, then let the converter operate the frequency to obtain the MPPT voltage, and then run P&O to ensure that it can output the maximum power.

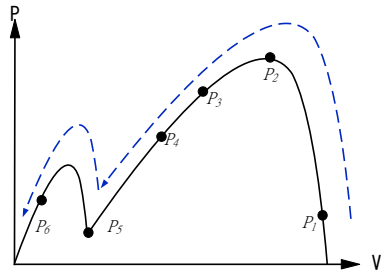

Figure 6. The P-V curve with the proposed GMPS method.

Figure 7 shows the global maximum power scan (GMPS) flow chart when the PV is operated in partial shadow. First, the voltage and current of the solar panel are measured. Second, the P-V curve is scanned by changing the switching frequency to obtain the MPPT

voltage. Third, the change between the last power and the new power is >50 W, and the P-V curve is scanned again to obtain the new MPPT voltage, so it can always operate at the maximum power point. If the power of each disturbance is <50 W, the traditional P&O method is executed to obtain the maximum power point.

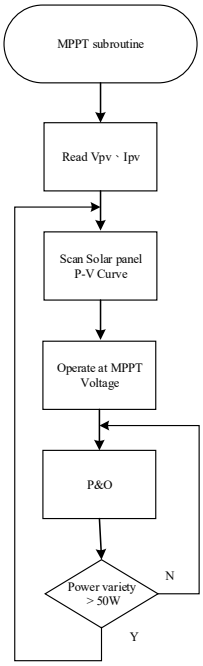

Figure 7. The flow chart of global maximum power scan (GMPS) under partial shading.

For DSP implementation, the function of enhanced capture, which has a very high sampling frequency, 150 MHz for Renesas RX62T, provides high-resolution voltage and current values of the solar panels. In this paper, the switching frequency range of the proposed LLC converter is 50 k~150 k, divided into 640 points, and each frequency change is 156.25 Hz. After sampling and averaging each A/D conversion, all 640 voltage and current values of the solar panel only need 0.16 s in total. Therefore, the total scan time only takes 0.16 s, and this method is only used when the power is turned on for the first time and the power change is greater than 50 W, so it will not affect the accuracy of the MPPT P&O disturbance.

3.2. Communication Scan Network (CSN) Interface

The system consists of two groups of three connected modules, so each module needs to communicate with the other modules. We set the first module as the master, then the other modules are the slave. The master module transmits the communication signal to the other ones with the RS-485 interface. The signal contained the voltage (V_{PV}), current (I_{PV}) and output voltage (V_o) of each module of the PV system. When one of the modules fails, the output voltage still regulates the same value by changing the voltage gain of the other normal modules. The RS-485 is a two wires half-duplex transmission, balanced signal pair and multipoint system. This communication network can be used over long distances in an electrically noisy environment. Multiple receivers may be connected to such a network in a linear fashion. These characteristics make RS-485 useful in the proposed six series-connected modules of the MPPT LLC Dc/Dc converters to achieve the global maximum power point and redundancy. Tables 1 and 2 show the protocol of the master sending a command to the other modules, and those modules receiving the command, then returning the data to the master, respectively. Figure 8 is the communication sequence diagram: the first module becomes the master. The first module prioritizes sending data, then asks the other modules to receive the data in sequence. When the first module fails,

then the second module becomes the master. The transmission time interval is 2 ms, so it takes a total of 16 ms to complete all communications and establish all voltage and current data for MPPT Dc/Dc converters. The proposed scan method will be completed within 16 ms, which is less than the time required for MPPT P&O disturbance. In other words, the proposed method in this paper has a redundant function without affecting the accuracy of MPPT.

Table 1. The protocol of the master command message.

Format	Number of Characters							
	1	**2**	**3**	**4**	**5**	**6**	**7**	**8**
Data Read	START	ID	Command (H)	Command (L)	Data (H)	Data (L)	CRC	END

Table 2. The protocol of slave receiving message.

Format	Number of Characters										
	1	**2**	**3**	**4**	**5**	**6**	**7**	**8**	**9**	**10**	**11**
Data Read	START	ID	Vpv (H)	Vpv (L)	Ipv (H)	Ipv (L)	Vo (H)	Vo (L)	Status	CRC	END

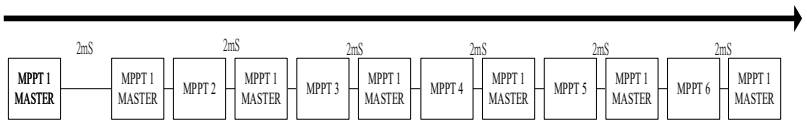

Figure 8. RS-485 communication time sequence diagram.

Figure 1 shows a schematic view of the studied, grid-connected, micro-grid systems located in National Tsing Hua University, Taiwan. The system consists of PV panels, DC grid, AC grid, battery packs, electronic breaker, STACOM, and a bi-directional inverter. However, the discussion is focused on the design and implementation of an MPPT and communication interface in this paper. The CAN bus is a robust vehicle bus standard, designed to allow microcontrollers and devices to communicate with each other's applications without a host computer, and it is a message-based-protocol. CAN bus has a good adjustment ability; it can add a net into the Network without changing the software and hardware. Table 3 shows the CAN bus data frame of the proposed system. The CAN bus interface is adopted to monitor the status of the devices in the proposed micro-grid system. Table 4 shows the data protocol with CAN bus interface. For example, the address 0x00~0x13 represents the status and data of two groups of three MPPT modules (DC_BUS_V−, DC_BUS_V+, PV1_I−, PV1_V−, PV1_I+, PV1_V+, PV2_I−, PV2_V−, PV2_I+, PV2_V+, PV3_I−, PV3_V−, PV3_I+, PV3_V+).

Table 3. CAN data frame.

START	ID	RTR	IDE	r0	DLC	DATA	CRC	END

Table 4. The data protocol with CAN bus interface.

ID	Name	Type	Data (8 Byte)							
			Byte 7	Byte 6	Byte 5	Byte 4	Byte 3	Byte 2	Byte 1	Byte 0
0x010	MPPT & Panel (1)	R	Status		0	0	DC_BUS_V−		DC_BUS_V+	
0x011	MPPT & Panel (2)	R	PV1_I−		PV1_V−		PV1_I+		PV1_V+	
0x012	MPPT & Panel (3)	R	PV2_I−		PV2_V−		PV2_I+		PV2_V+	
0x013	MPPT & Panel (4)	R	PV3_I−		PV3_V−		PV3_I+		PV3_V+	
0x020	Charger/Discharger (1)	R	Status		SOC		DC_BUS_V−		DC_BUS_V+	
0x021	Charger/Discharger (2)	R	0	0	0	0	DC_BUS_I−		DC_BUS_I+	
0x022	Charger/Discharger (3)	R	Battery_I−		Battery_I+		Battery_V−		Battery_V+	
0x02F	Charger/Discharger (4)	R	0	0	0	0	0	0	MODE	
0x12F	Charger/Discharger (4)	W	0	0	0	0	0	0	MODE	
0x040	STATCOM	R	Status		PF		Real Power		Reactive Power	
0x041	STATCOM	R	Vp		Vn		Vh2		Vh3	
0x042	STATCOM	R	Vh4		Vh5		Vh6		Vh7	
0x043	STATCOM	R	0	0	0	0	w		Vh8	
0x04F	STATCOM	R	0	0	Q mode		In mode		H mode	
0x14F	STATCOM	W	0	0	Q mode		In mode		H mode	
0x050	Bi-directional inverter (1)	R	Status		0	0	DC_BUS_V−		DC_BUS_V+	
0x051	Bi-directional inverter (2)	R	AC_I		AC_V		DC_BUS_I−		DC_BUS_I+	
0x05F	Bi-directional inverter (3)	R	0	0	0	0	0	0	MODE	
0x15F	Bi-directional inverter (3)	W	0	0	0	0	0	0	MODE	
0x06F	Electronic Breaker	R	Status		EB3		EB2		EB1	
0x16F	Electronic Breaker	W	0	0	EB3		EB2		EB1	

4. Experimental Results

4.1. LLC Converter Hardware Implementation and Measured Results

A 1 kW LLC Dc/Dc converter is implemented and tested to verify the accuracy with a Renesas RX62T micro-controller. The design specification of the DC/DC converter is listed in Table 5. Experimental results are measured and shown in Figure 9a,b, which shows the measured key waveforms for the system operating at 500 W and 1000 W, with the voltage V_{DS} and voltage V_{GS} of the switches. From the measured results, we can see that the zero voltage switching (ZVS) is achieved for the resonant converter. Additionally, the measured output power vs. efficiency curve is shown in Figure 10. The efficiencies remain above 84% when the system is operated from a light load to a heavy load. The LLC converter is suitable for use when the converter is operated for a high input voltage and low output voltage and high current output because the active switch of the primary side works in ZVS and the diode of the secondary side works in ZCS. The circuit architecture proposed in this paper is aimed toward high-power systems, that is, input with a high voltage and output with a low voltage (large current). However, the power level of the experimental prototype is low, so it cannot show the advantages of LLC.

Table 5. The specification of LLC DC/DC converter.

Item	Specification
Input Voltage	112 V~144 V
Output Voltage	380 V
Output Power	6 kW (6 modules)
Operating Frequency	50 kHz~150 kHz
MPPT tracking efficiency	>99%
efficiency	>85%

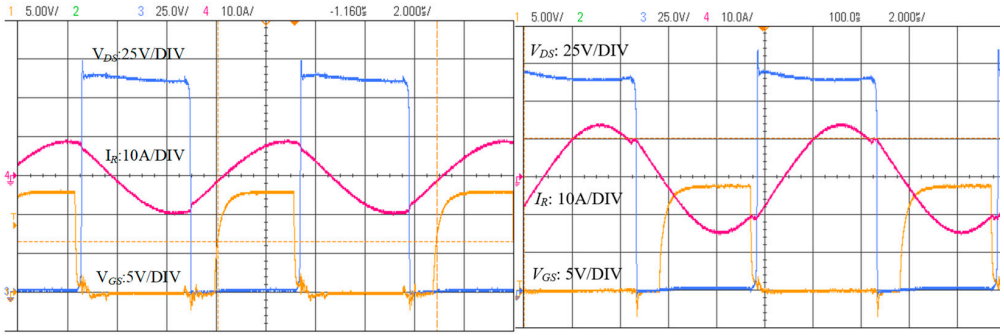

Figure 9. The measured waveforms of the LLC converter when the system is operated at (**a**) 500 W (**b**) 1 kW.

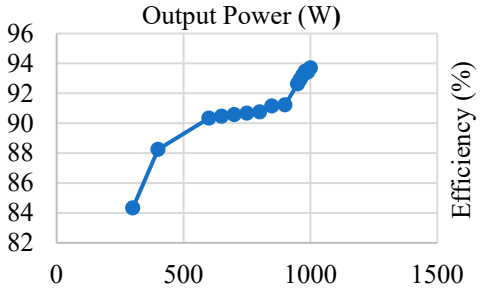

Figure 10. Output power vs. efficiency curve.

Figure 11a,b demonstrate maximum power tracking with irradiation of 1000 W/m^2, with a tracking accuracy of 99%. Additionally, the tracking curve of the simulated solar energy under two different partial shading (PS) conditions is shown in Figure 12a,b. The experimental results show that the GMPS method can track the maximum power point for different irradiations and PS conditions with the proposed global P-V MPPT methods.

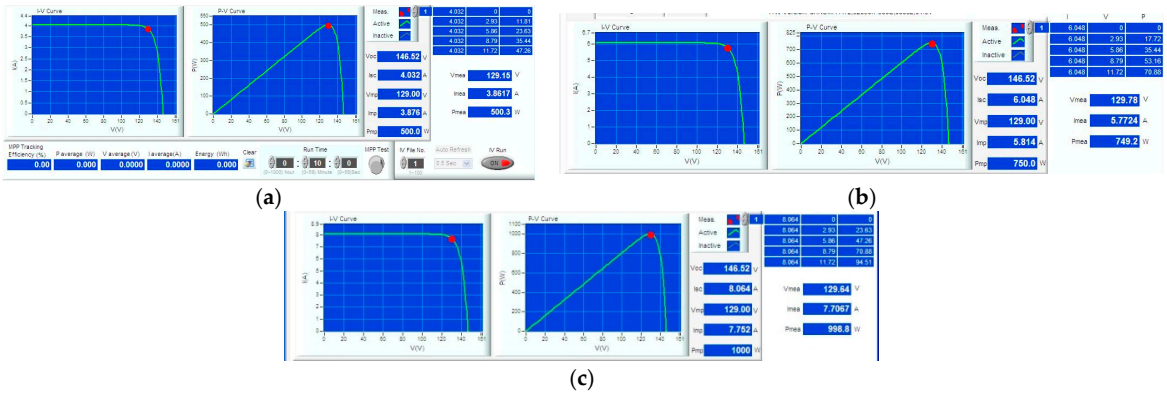

Figure 11. The tracking point of I-V and P-V curves under 1000 W/m^2 (**a**) 500 W (**b**) 750 W (**c**) 1000 W.

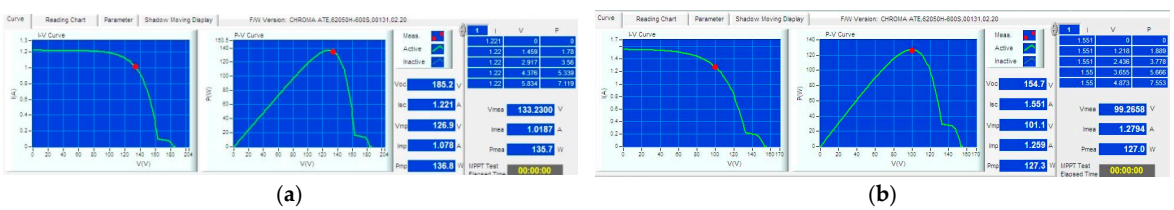

Figure 12. The tracking point of I-V and P-V curves under partial shading (**a**) condition 1, (**b**) condition 2.

4.2. Communication Scan Network (CSN)

The system designed in this paper is a series connection of multiple groups. As the output is connected in series, the output voltage of each group needs to be added. However, the output voltage is too high and the internal communication time needs to be quite immediate. RS-485 is used for this research. The internal systems communicate with each other. As RS-485 is a 2-wire half-duplex, after sending a communication request with master, other systems will send back system data on the same bus, including solar panel voltage, current, and output voltage, which are sent in turn in the order of the system number. Figure 13 shows the communication signals on the internal RS-485 bus. Each group of signals is sent at an interval of 2 ms. There are six groups in total. After the six groups have been sent, the first group will send them again. This cycle is repeated and the circuit data are returned in real time. The immediacy of the circuit is achieved. Figure 13 shows RS-485 communication waveform; we set MPPT1 as the master, then MPPT1 sends a command to ask the others to return the data and save it. The red waveform shows the master transmit and receive condition (high means transmit, low means receive), and the yellow one is RS-485 waveform. We only connect with MPPT1, MPPT3 and MPPT4, so there is no data return from MPPT2, MPPT5 and MPPT6.

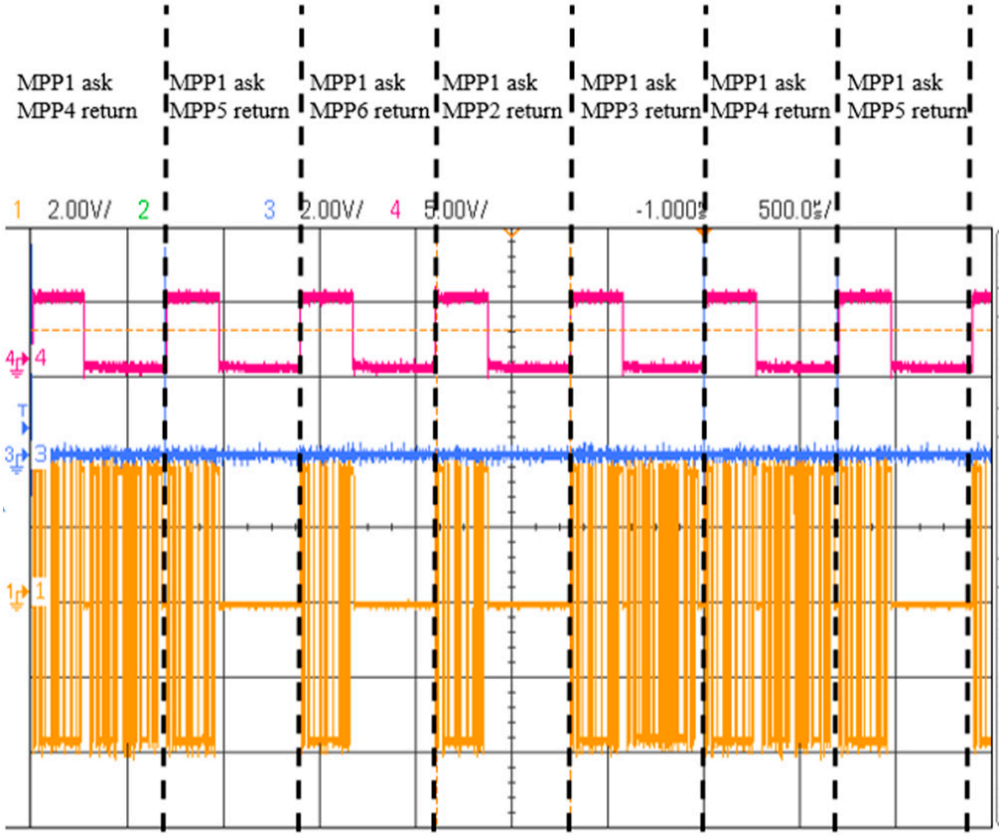

Figure 13. RS-485 communication waveform.

In this paper, six groups of systems are connected in series. The internal communication uses RS-485 as the communication interface. This research uses LabVIEW as the monitoring interface. Each group of information is read from the RS-485 bus and displayed on the interface, including the voltage and current of the solar panel, which were displayed after adding the total output of the three groups. When scanning the solar panel curve, the solar panel curve can also be displayed on the interface. Figure 14 shows the LabVIEW interface. The left side of the interface is the solar panel voltage. The currents are arranged in sequence according to the number of each group. The VDC_BUS voltage is also the sum

of the first three groups of output voltages and the sum of the last three groups of output voltages. On the right, the solar panel characteristic curve is recorded while scanning, and the solar panel voltage–current curve and voltage–power curve are drawn.

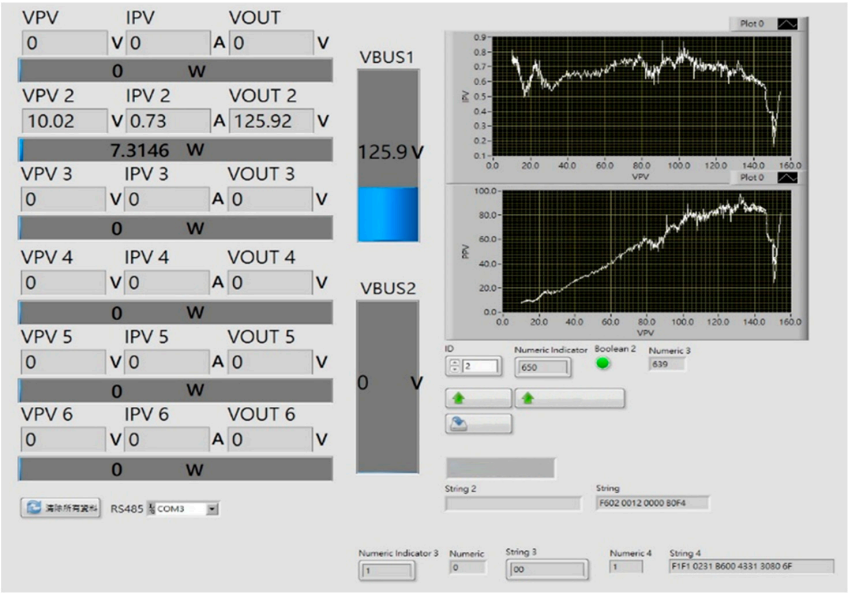

Figure 14. LabVIEW monitoring screen.

4.3. High Reliability

To improve the system's reliability, each module uses the RS-485 interface to communicate, as in section B, to ensure that proposed system works normally. For example, if module 3 fails, the modules will immediately protect and inform other modules using the RS-485 communication scan network. Therefore, other modules will change the operating frequency of the LLC converter to change the output voltage. However, the total series output voltage is controlled by the power of the grid inverter circuit. This paper shows that the series connection of the modules can still stabilize 380 V and achieve the MPPT feature when one of the modules fails.

When the system is operated in normal mode, we connect three 1 kW LLC converter in series so that DC_BUS voltage can output 380 V. Figure 15a,b show the transient and steady output voltages of three modules, respectively. From the measured results, we can see that each module's voltage is about 126 V, so three modules in series can output 380 V. Additionally, when one module fails, the system still needs to regulate 380 V, as shown in Figure 16. Figure 17a,b show the transient and steady output voltages of three modules, respectively. Figure 17b shows the output voltages of each module when the system is operated in abnormal mode; we can see that two module's voltages, V_{O1} and $V_{O2,}$ rise to about 190 V, so that three modules in series can still regulate at 380 V. A photograph of the proposed 6 kW LLC converters is shown in Figure 18.

This paper uses the LabVIEW interface to connect the system. The reading method aims to connect the RS-485 bus to the receiving end, read the data on the RS-485 bus, and then process them with software and send them to the computer database. The information includes the voltage and current of the solar illuminance meter and the solar panel. The method of reading the power is calculated from the voltage and current read. Compared with the curve in the solar panel power and illuminance, the output voltage is output at the normal working output voltage of 126 V. Figure 19 shows the measured data for input power, output voltage and solar irradiation of the master module on the RS-485 bus. The output power of the solar panel follows the change in the irradiation, which verifies the correctness of the proposed MPPT method.

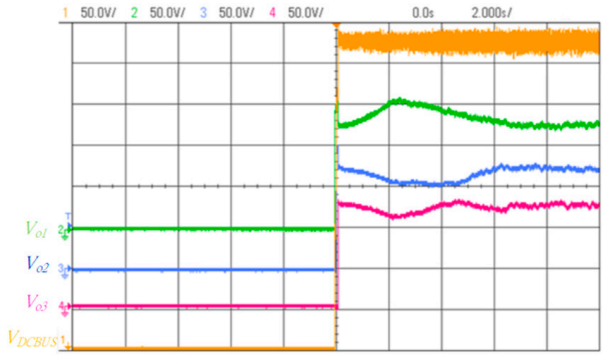

(V_{O1}: 50 V/ div, V_{O2}: 50 V/ div, V_{O3}: 50 V/ div, V_{DCBUS}: 50 V/ div, Time: 2 s/ div)

(**a**)

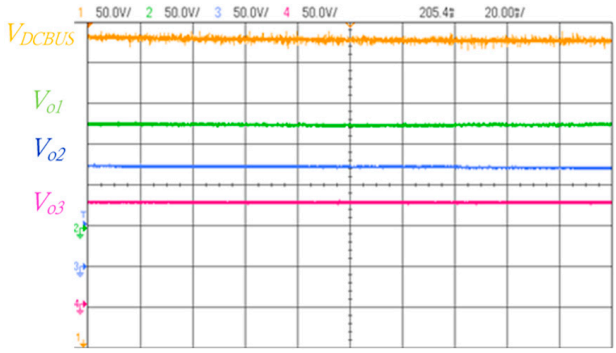

(V_{O1}: 50 V/ div, V_{O2}: 50 V/ div, V_{O3}: 50 V/ div, V_{DCBUS}: 50 V/ div, Time: 20 ms/ div)

(**b**)

Figure 15. The output voltages of three modules when the system is operated in normal mode (**a**) transient (**b**) steady state.

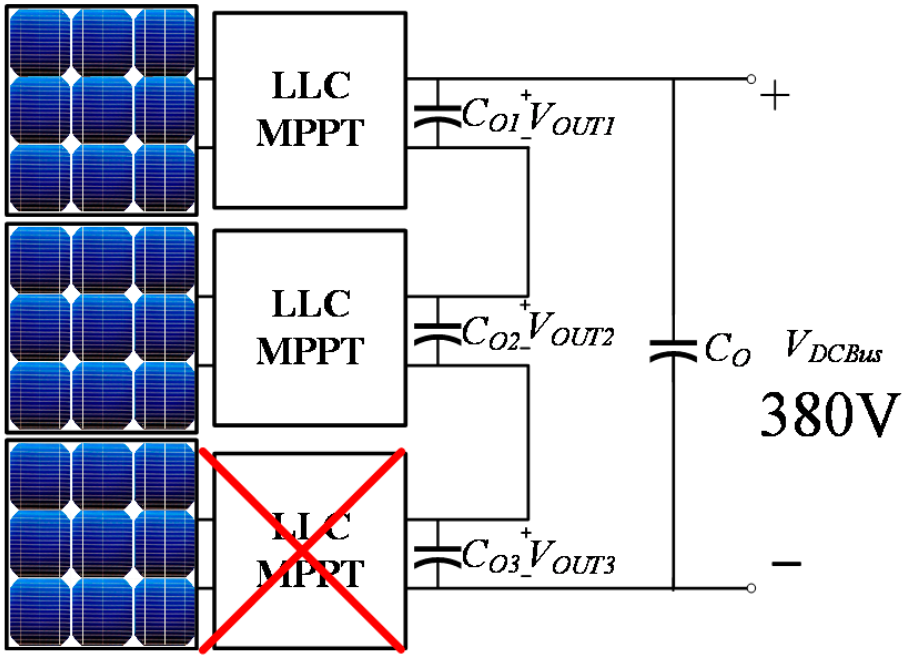

Figure 16. The system is operated in abnormal mode.

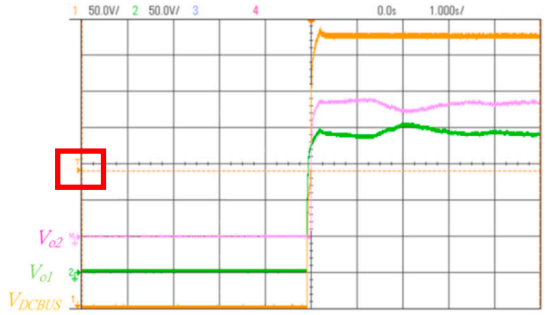

(V_{O1}: 50 V/div, V_{O2}: 50 V/div, V_{DCBUS}: 50 V/div, Time: 2 s/div)

(**a**)

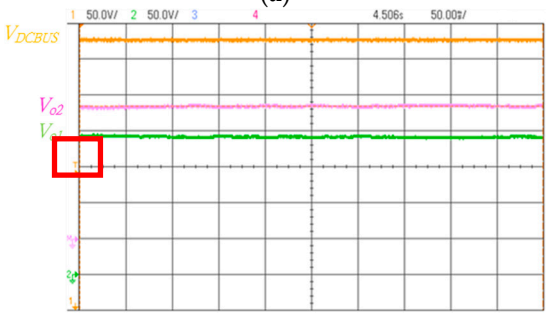

(V_{O1}: 50 V/div, V_{O2}: 50 V/div, V_{DCBUS}: 50 V/div, Time: 20 ms/div)

(**b**)

Figure 17. The output voltages of three modules when the system is operated in abnormal mode (**a**) transient (**b**) steady state.

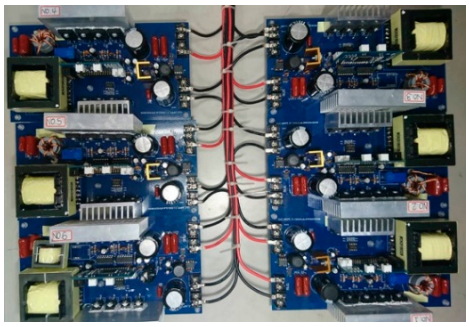

Figure 18. The photograph of the proposed 6 kW LLC converters.

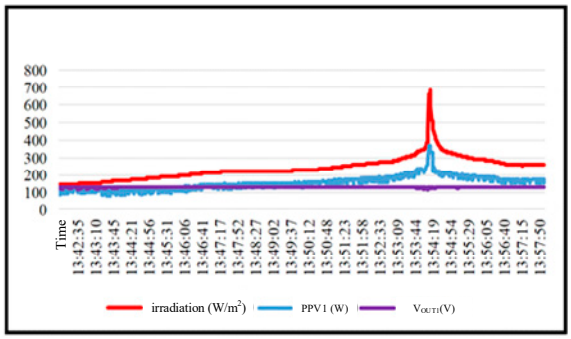

Figure 19. Irradiation vs. solar panel power and voltage.

The proposed communication scan network (CSN) using LabVIEW graphic software was implemented to control and monitor the proposed microgrid system. The communication interface for each subsystem includes CAN BUS. When receiving system commands

from the controller of CSN, each unit executed corresponding actions and replied with signals to CSN. The system converted the signals into monitoring data for the display and database documentation to realize a CSN. The proposed connected MPPT LLC Dc/Dc converters used RS-485 network topology for half-duplex network communication. The RS-485 network topology consists of RS-232 and UART of each LLC module to form the communication interface. Figure 20 shows the measured waveforms for address 0x10 and 0x11 with CAN bus. With two power sources, solar cell, battery, bi-directional inverter, EB and STACOM are connected and implemented in a PV micro-grid system using LabVIEW, as shown in Figure 21. Figure 22 shows a photograph of integrated testing for the proposed microgrid system.

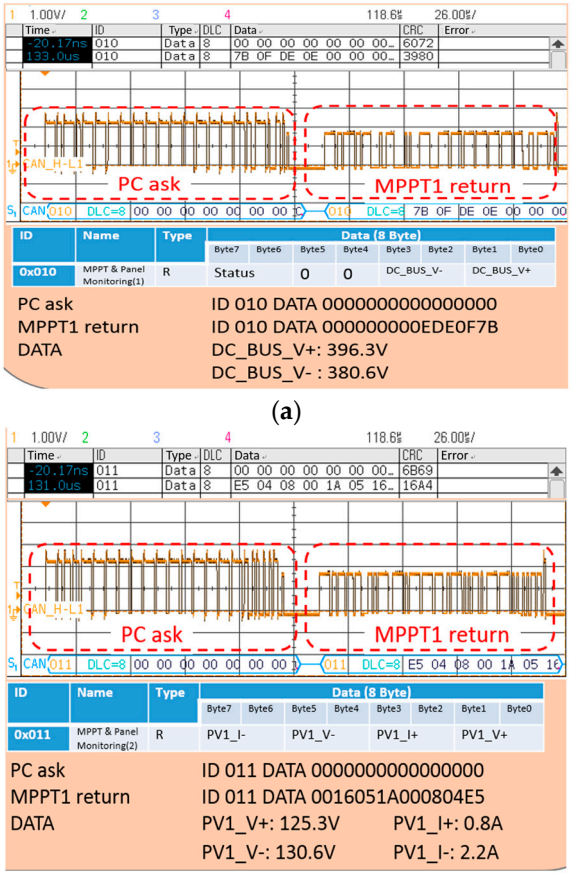

Figure 20. CAN communication waveform (**a**) ID: 0x10 (**b**) ID: 0x11.

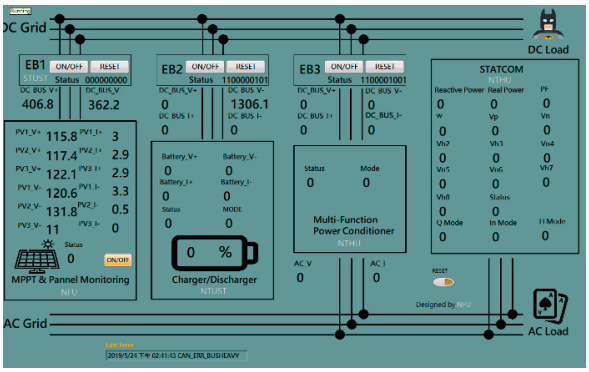

Figure 21. LabVIEW monitoring screen of with communication scan network.

Figure 22. The photograph of the proposed PV micro-grid prototype system with communication scan network.

5. Conclusions

As verified through experimental results, the global maximum power point, high flexibility and redundancy of the proposed system with a communication scan network were achieved for the PV micro-grid system in this paper. The design output voltage of LLC converter was fixed to ±380 V, and, using a global maximum power scan control, MPPT achieved, at the maximum point, a converter efficiency as high as 94%, and an MPPT accuracy of 99.9% when the system is operated at full load. Therefore, the isolated soft-switching LLC converter is adopted to achieve high efficiency and eliminate the leakage current for a PV grid-tied system.

Additionally, the output voltage of the proposed LLC modules can still stabilize 380 V when one of the series-connected modules fails, and achieve the global MPPT feature under partially shaded conditions with the proposed communication scan network. This paper proposes a series-connected architecture with frequency controls to complete the global maximum power point of the solar panel. Each independent LLC-isolated maximum power tracker can use RS-485 communication to determine the range of its switching frequency and achieve the purpose of redundancy. The number of panels can be increased as per the voltage and power requirements.

From the experimental results, we can see that the proposed power scan control method and series-connected LLC power topology are the accuracy and feasibility of the PV micro-grid system with RS-485 and CAN bus interface in this paper. In short, this paper proposes a novel method that makes full use of the advantages of the DSP chip's computing speed, and makes full use of the software to achieve a global MPPT, high flexibility and high reliability.

Author Contributions: Y.-K.C., H.-W.H. and Y.-S.C. conceived the presented idea, designed, experimented and wrote this article; Y.-K.C. and C.-C.S. supervised the findings of this work; All authors have read and agreed to the published version of the manuscript.

Funding: This research was funded by the Ministry of Science and Technology, Taiwan, R.O.C., grant number MOST 110-2221-E-150-008, MOST 110-2221-E-150 -041and MOST 110-2622-8-005-005-TE1.

Institutional Review Board Statement: Not applicable.

Informed Consent Statement: Not applicable.

Data Availability Statement: Not applicable.

Conflicts of Interest: The authors declare no conflict of interest.

References

1. European Photovoltaic Industry Association. Global Market Outlook for Solar Power 2015–2019. Available online: www.epia.org (accessed on 1 May 2021).
2. Salameh, Z.; Dagher, F.; Lynch, W.A. Step-Down Maximum Power Point Tracker for Photovoltaic System. *Sol. Energy* **1991**, *46*, 278–282. [CrossRef]
3. Enslin, J.H.R. Maximum Power Point Tracking: A Cost Saving Necessity in Solar Energy System. *IEEE Trans. Ind. Electron. Soc. Conf.* **1990**, *2*, 1073–1077.
4. Hsieh, G.C.; Tsai, C.Y.; Hsieh, H.I. Photovoltaic power-increment-aided incremental-conductance maximum power point tracking using viable frequency and duty controls. In Proceedings of the 3rd International Symposium on Power Electronics for Distributed Generation Systems, Aalborg, Denmark, 25–28 June 2012; pp. 542–549.
5. Shahana, P.S.; Linus, R.M. Modified Maximum Power Point Tracking for PV System Using Single Switch DC/DC Converter. In Proceedings of the International Conference on Electrical, Electronics, and Optimization Techniques (ICEEOT), Chennai, India, 3–5 March 2016; pp. 3156–3160.
6. Hussein, K.H.; Muta, I.; Hoshino, T.; Osakada, M. Maximum photovoltaic power tracking: An algorithm for rapidly changing atmospheric conditions. *IEE Proc. Gener. Transm. Distrib.* **1995**, *142*, 59–64. [CrossRef]
7. Sankar, R.; Velladurai, S.; Rajarajan, R.; Thulasi, J.A. II. PV System Description. Maximum Power Extraction in PV System using Fuzzy Logic and Dual MPPT Control. In Proceedings of the International Conference on Energy, Communication, Data Analytics and Soft Computing (ICECDS), Chennai, India, 1–2 August 2017; pp. 3764–3769.
8. Elewa, A.; Elkholy, M.M.; El-arini, M. Adaptive MPPT for PV systems under partial shadow condition and different loads using advanced optimization techniques. In Proceedings of the 2017 Nineteenth International Middle East Power Systems Conference (MEPCON), Cairo, Egypt, 19–21 December 2017; pp. 152–162.
9. Gong, H.J.; Yan, F.; Zhang, C.F.; Zou, Y.Q. An enhanced MPPT approach under partial shadowing condition (PSC) combining fiatness control and direct P&O method. In Proceedings of the 2016 35th Chinese Control Conference (CCC), Chengdu, China, 27–29 July 2016; pp. 8556–8561.
10. Hsieh, G.C.; Chen, H.L.; Chen, Y.; Tsai, C.M.; Shyu, S.S. Variable frequency controlled incremental conductance derived MPPT photovoltaic stand-along DC bus system. In Proceedings of the 2008 Twenty-Third Annual IEEE Applied Power Electronics Conference and Exposition, Austin, TX, USA, 24–28 February 2008; pp. 70–75.
11. Zhang, Q.; Hu, C.; Chen, L.; Amirahmadi, A.; Kutkut, N.; Shen, Z.J.; Batarseh, I. A Center Point Iteration MPPT Method with Application on the Frequency-Modulated LLC Microinverter. *IEEE Trans. Power Electron.* **2014**, *29*, 1262–1274. [CrossRef]
12. Başoğlu, M.E. An Improved 0.8 VOC Model Based GMPPT Technique for Module Level Photovoltaic Power Optimizers. *IEEE Trans. Ind. Appl.* **2019**, *55*, 1913–1921. [CrossRef]
13. Goud, J.S.; Kalpana, R.; Singh, B. A Hybrid Global Maximum Power Point Tracking Technique with Fast Convergence Speed for Partial-Shaded PV Systems. *IEEE Trans. Ind. Appl.* **2018**, *54*, 5367–5376. [CrossRef]
14. Ahmad, W.; Khan, Z.A.; Khan, U.H.; Alam, Z.; Qasuria, H.T.; Mustafa, E. Neural Network based Robust Nonlinear GMPPT Control Approach for Partially Shadow Conditions of Solar Energy System. In Proceedings of the International Conference on Emerging Trends in Smart Technologies (ICETST), Karachi, Pakistan, 26–27 March 2020.
15. Deboucha, H.; Shams, I.; Belaid, S.L.; Mekhilef, S. A Fast GMPPT Scheme Based on Collaborative Swarm Algorithm for Partially Shaded Photovoltaic System. *IEEE J. Emerg. Sel. Top. Power Electron.* **2021**, *9*, 5571–5580. [CrossRef]
16. Kjaer, S.B.; Pedersen, J.K.; Blaabjerg, F. A Review of Single-Phase Grid-Connected Inverters for Photovoltaic Modules. *IEEE Trans. Ind. Appl.* **2005**, *41*, 1292–1306. [CrossRef]
17. Rodriguez, J.; Franquelo, L.G.; Kouro, S.; Leon, J.I.; Portillo, R.; Prats, M.A.M.; Perez, M.A. Multilevel Converters: An Enabling Technology for High-Power Applications. *Proc. IEEE* **2009**, *97*, 1786–1817. [CrossRef]
18. Meinhardt, M.; Cramer, G.; Burger, B.; Zacharias, P. Multi-string Converter with Reduced Specific Costs and Enhanced Functionality. *Sol. Energy* **2001**, *69*, 217.
19. Rouf, A.; Nag, S.S. An Improved PV to Isolated Port Differential Power Processing Architecture for Solar PV Applications. In Proceedings of the 2021 IEEE Energy Conversion Congress and Exposition (ECCE), Vancouver, BC, Canada, 10–14 October 2021; pp. 130–136.
20. Kanathipan, K.; Lam, J. A High Voltage Gain Isolated PV Micro-converter With a Single-voltage Maximum Power Point Tracking Control Loop for DC Micro-grid Systems. *IEEE J. Emerg. Sel. Top. Ind. Electron.* **2021**, 1. [CrossRef]